JOURNAL OF CATALYSIS 103, 65–78 (1987)

Isotopic Exchange Measurements of the Rates of Adsorption/Desorption and Interconversion of CO and CO_2 over Chromia-Promoted Magnetite: Implications for Water-Gas Shift

M. TINKLE[1] AND J. A. DUMESIC[2]

Department of Chemical Engineering, University of Wisconsin, Madison, Wisconsin 53706

Received March 23, 1986; revised July 22, 1986

Isotopic exchange measurements were used to investigate the adsorption/desorption and interconversion of CO and CO_2 on chromia-promoted magnetite at 565 and 627 K. The interconversion between CO and CO_2 was shown to take place through surface adsorbed species. Furthermore, the rate of interconversion was limited by the rates of adsorption/desorption, indicating either that adsorbed CO and CO_2 are in equilibrium on the surface or that the adsorption of CO and CO_2 leads to the same surface species, e.g., a surface carbonate species. A kinetic model for the water-gas shift over magnetite is proposed, and the results of the isotopic exchange measurements and volumetric adsorption data are used to estimate the rate and equilibrium constants for this model.

INTRODUCTION

Despite the fact that chromia-promoted magnetite is an effective water-gas shift catalyst, the mechanism for this reaction has not yet been unambiguously defined. Two types of catalytic roles of magnetite have been suggested, as reviewed elsewhere (*1*): that the catalyst provides a surface for adsorption and interaction of the water-gas shift reactant species to form product species followed by desorption, and that the catalyst participates as an oxygen transfer medium and is alternately oxidized and reduced through a "regenerative" mechanism. Previous studies have addressed both the adsorptive properties (*2*) and the oxygen transfer properties (*3*) of chromia-promoted magnetite. The objectives of the present work are to determine whether these adsorptive and oxygen transfer properties are related, and to compare the relative rates of adsorption/desorption with the rates of interconversion of CO and CO_2 under equilibrium conditions. This will be accomplished through the use of isotopically labeled species. Finally, these results will be used to propose a mechanism and rate expression for the water-gas shift reaction over chromia-promoted magnetite.

It has been proposed previously that the regenerative mechanism is the dominant pathway for water-gas shift over chromia-promoted magnetite (*3*). The regenerative half-reactions which combine to give the overall reaction have typically been written as Rideal–Eley steps:

$$CO(g) + O^* \rightleftarrows CO_2(g) + * \quad (1)$$

$$H_2O(g) + * \rightleftarrows H_2(g) + O^*, \quad (2)$$

where O* represents a reducible oxygen-containing site on the surface and * an oxidizable anion vacancy. Indeed, a rate expression based on this mechanism (*4*) has been shown to give a good fit to water-gas shift kinetic data (*5*). Recent work by Rethwisch and Dumesic (*6*) has indicated that the high activity of magnetite for water-gas shift relative to other oxides is linked to the variable oxidation state of iron in the catalyst, which facilitates surface oxygen transfer.

[1] Present address: Shell Development Company, P.O. Box 1380, Houston, Texas 77251-1380.

[2] To whom correspondence should be addressed.

0021-9517/87 $3.00

It has been suggested, however, that an expression of a regenerative mechanism more realistic than the Rideal–Eley scheme might involve adsorbed intermediates (*7*, *8*). Significant amounts of adsorbed species are present on the surface of magnetite under water-gas shift conditions. In fact, Lund and Dumesic (*9*) concluded that catalysts not active for adsorption of CO and CO_2 are not active for water-gas shift. Accordingly, the importance of adsorption phenomena in the regenerative mechanism will be investigated in the present study.

It has been shown (*3*, *10*) that the oxygen content of chromia-promoted magnetite varies according to the thermodynamic oxygen activity of the gas phase in equilibrium with the solid. In general, this thermodynamic activity at a given temperature is proportional to the $CO_2:CO$ or $H_2O:H_2$ partial pressure ratios. This behavior was employed by Kubsh and Dumesic (*3*) to study gravimetrically the rates of oxidation and reduction of magnetite as a function of the oxygen content of the catalyst. While the importance of the regenerative mechanism was demonstrated, the role of adsorbed species in regenerative oxygen transfer reactions could not be clearly elucidated since adsorbed species and surface oxygen could not be distinguished gravimetrically. The present study effects the separation between adsorbed species and surface oxygen through the use of ^{13}C as an isotopic tracer in CO_2/CO gas mixtures in equilibrium with chromia-promoted magnetite.

Materials and Procedures

Isotopic exchange measurements were carried out under equilibrium conditions in CO/CO_2 mixtures. The catalyst was a commercial chromia-promoted (7% chromia) magnetite obtained from Haldor Topsøe A/S (SK-12). Four different samples were studied: an unsieved, ground, 1.9-g sample; two 1.9-g samples, 70–100 mesh (0.149–0.210 mm) in size; and a 1.5-g sample, finer than 200 mesh (0.074 mm). The different sample granule sizes were used to determine whether pore diffusion was limiting under the conditions of the experiments.

Each sample was pretreated as prescribed by Lund *et al.* (*11*). First the sample was reduced for 30 ks (8 h) or longer in a flowing CO/CO_2 gas mixture ($CO:CO_2 = 7:1$) at 653 K. Following reduction, the sample was evacuated for 3.6 ks. During the first 2.7 ks of the evacuation, the temperature was maintained at 653 K. During the final 0.9 ks of the evacuation, the temperature was lowered to the temperature under investigation (563–630 K). The final evacuation pressure was approximately 1×10^{-3} Pa (1×10^{-5} Torr).

A schematic diagram of the glass system used is shown in Fig. 1. After the catalyst was evacuated, the Pyrex sample cell was isolated, and a mixture of CO and CO_2 (natural isotopes) was prepared in the dosing manifold. First, the desired amount of CO_2 was admitted to the manifold. The CO_2 was then frozen in an extension of the manifold which was immersed in liquid nitrogen, and the amount of CO required to attain the planned total dosing pressure and composition was added to the manifold. The liquid nitrogen was then removed from the extension, stopcock A was opened, and the system was allowed to reach equilibrium overnight.

After this equilibrium state was reached,

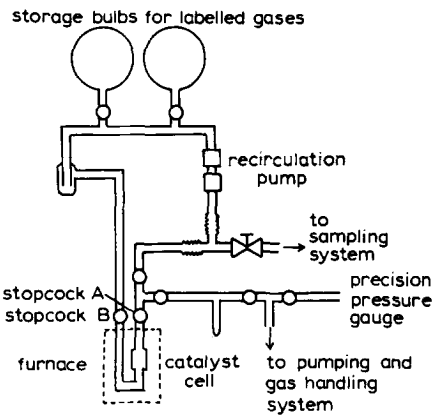

FIG. 1. Schematic of isotopic exchange apparatus.

the cell was isolated by closing stopcock A, leaving in the cell a small amount of the gas mixture. The composition of the mixture in the manifold was determined by freezing the CO_2 in the gas phase by again immersing the manifold extension in liquid nitrogen and comparing the pressures before and after the freezing. Thus the initial and final pressures and compositions were measured, and the amounts of CO and CO_2 remaining in the cell both in the gas phase and adsorbed on the catalyst surface could be calculated (*2*). The total amount adsorbed was determined volumetrically using the ideal gas law. Equilibrium pressures were in the 2.8 kPa (21 Torr; 1 Torr = 133.3 Pa) range.

The next step in the experiment was to prepare in the above manner an isotopically labeled CO/CO_2 mixture in the exchange loop with composition and pressure equal to that in the catalyst cell. Either the CO or the CO_2 in this mixture was labeled with ^{13}C. Stopcocks A and B were opened, and the glass circulation pump was turned on to mix the gas in the loop. In this way, the exchange of the labeled species in the gas phase with species adsorbed on the surface could be observed and measured, yielding the equilibrium rates of adsorption and desorption under the experimental conditions. Additionally, the rate of interconversion between CO and CO_2 through the CO/CO_2 half of the regenerative mechanism (Eq. (1)) could be measured.

A small amount of the gas in the system was diverted through a leak valve to the sampling system. A quadrupole mass spectrometer (UTI Model 100C) was used to measure signals from ^{12}CO, ^{13}CO, $^{12}CO_2$, and $^{13}CO_2$. The mass spectrometer was controlled by a Peak Programmer Selector (UTI Model 2054), which sampled the four channels. The signals from the mass spectrometer were used to calculate the fraction of CO labeled and the fraction of CO_2 labeled as functions of time.

The CO/CO_2 mixture used for the catalyst pretreatment was obtained from Matheson. Iron carbonyl in the mixture was decomposed by passing the mixture through a heated tube (T = 653 K) and a glass frit prior to passing the mixture through the catalyst cell. Natural CO (CP grade, 99.5% pure, minimum) and CO_2 (bone dry grade, 99.8% pure, minimum) were also obtained from Matheson. The CO was further purified by passage over hot copper turnings (523 K) followed by passage through an activated molecular sieve trap (Davison, 13×) at 195 K. The CO_2 was purified by freezing in liquid nitrogen at 77 K and evacuating to 10^{-4} Pa 10^{-6} Torr). The purified gases were stored in 5-dm^3 storage bulbs in the glass vacuum system.

Carbon-13 labeled CO and CO_2 were obtained from Stohler-KOR isotopes in 101 kPa (1 atm), 0.1-dm^3 glass bulbs and they were used without further purification. Both the CO and CO_2 contained 99% ^{13}C.

Isotopic Exchange Measurements

The possible effects of the gas mixing time in the cell and loop and of pore diffusion within the catalyst were investigated in this study of adsorption/desorption and interconversion of CO and CO_2. An experiment where silica replaced magnetite in the cell was run to test the effects of mixing time in the system on isotopic exchange results. The mixing experiment was run under conditions comparable to the isotopic exchange experiments, under which silica does not adsorb CO or CO_2 to a measurable extent (*12*). The results showed that mixing occurs within 10 s, a time much shorter than the characteristic times for isotopic exchange over magnetite. It is therefore concluded that mixing effects in the isotopic exchange experiment are negligible.

Estimations of the Thiele modulus for isotopic exchange showed that the effects of pore diffusion should not influence the observed reaction rates (*13*). This result was verified by observing that the measured exchange rates were independent of the magnetite particle size for the different ground samples. It should also be noted

that the kinetic isotope effect between ^{12}C and ^{13}C is negligible for the purposes of this study (*14*).

The present isotopic exchange experiments start with the catalyst in equilibrium with a CO/CO_2 gas mixture composed of natural isotopes. A CO/CO_2 mixture containing either labeled CO or labeled CO_2 of equal total pressure and composition is then exposed to the catalyst, and the exchange of the different species under equilibrium conditions is observed. For example, if the experiment is initiated with labeled ^{13}CO and natural CO_2 in the gas phase, then ^{13}CO can exchange with ^{12}CO adsorbed on the catalyst and it can react with oxygen on the catalyst surface, generating $^{13}CO_2$. Because the experiment is carried out under equilibrium conditions, the total amounts of both CO and CO_2 in the gas phase, the amount of oxygen on the catalyst surface, and the total amount of each species adsorbed on the surface are constant throughout the experiment. These quantities are known, since the initial and final pressures and volumes of the natural CO/CO_2 mixture used to equilibrate the system are known, as are the pressure, volume, and composition of the exchange mixture. If the transfer of oxygen between CO, CO_2, and the catalyst surface occurs through an adsorbed intermediate, the following equilibria are in effect:

$$CO + \alpha \underset{k_1'}{\overset{k_1}{\rightleftarrows}} CO \cdot \alpha \qquad (3)$$

$$CO_2 + \beta \underset{k_2'}{\overset{k_2}{\rightleftarrows}} CO_2 \cdot \beta \qquad (4)$$

$$CO \cdot \alpha \underset{k_3'}{\overset{k_3}{\rightleftarrows}} CO_2 \cdot \beta \qquad (5)$$

Here, α and β represent adsorption sites for CO and CO_2, respectively, on the catalyst surface. A mass balance for Eq. (5) requires that an α site is a β site containing an additional oxygen atom. The forward and reverse reaction rate constants for each step are represented by k_i and k_i', respectively. When brackets around a species are used to represent concentrations, the equilibrium rates of the above reaction steps R_1, R_2, and R_3 can be expressed as

$$R_1 = k_1[CO][\alpha] = k_1'[CO \cdot \alpha] \qquad (6)$$

$$R_2 = k_2[CO_2][\beta] = k_2'[CO_2 \cdot \beta] \qquad (7)$$

$$R_3 = k_3[CO \cdot \alpha] = k_3'[CO_2 \cdot \beta]. \qquad (8)$$

R_1, R_2, and R_3 are measured in μmol/s. To analyze the data, the fraction of each carbon-containing species which is labeled is considered. The fractions of gas phase CO and CO_2 labeled with ^{13}C are denoted by G_{CO} and G_{CO_2}, respectively; e.g.,

$$G_{CO} = [^{13}CO]/([^{13}CO] + [^{12}CO]). \qquad (9)$$

Similarly, the labeled mole fractions of $[CO \cdot \alpha]$ and $[CO_2 \cdot \beta]$ are denoted by A_{CO} and A_{CO_2}, respectively; e.g.,

$$A_{CO} = [^{13}CO \cdot \alpha]/([^{13}CO \cdot \alpha] + [^{12}CO \cdot \alpha]). \qquad (10)$$

Thus, the changes in the amounts of labeled CO and CO_2 in the gas phase with respect to time may be written:

$$\frac{d[^{13}CO]}{dt} = [CO]\frac{dG_{CO}}{dt} = R_1(A_{CO} - G_{CO}) \qquad (11)$$

$$\frac{d[^{13}CO_2]}{dt} = [CO_2]\frac{dG_{CO_2}}{dt} = R_2(A_{CO_2} - G_{CO_2}). \qquad (12)$$

The rate of change of the labeled adsorbed CO is

$$\frac{d[^{13}CO \cdot \alpha]}{dt} = [CO \cdot \alpha]\frac{dA_{CO}}{dt} = R_1(G_{CO} - A_{CO}) + R_3(A_{CO_2} - A_{CO}). \qquad (13)$$

The analogous rate equation for labeled CO_2 is not necessary because the equilibrium mass balances are also known. The amount of ^{13}C in the system is constant, and the amounts of CO and CO_2 in the gas phase and adsorbed on the catalyst remain at the amounts measured at the beginning of the experiment. If $[^{13}C]_{TOT}$ represents the known amount of labeled carbon species in-

troduced at the beginning of the experiment, then the relationship

$$[^{13}C]_{TOT} = G_{CO}[CO] + G_{CO_2}[CO_2] + A_{CO}[CO \cdot \alpha] + A_{CO_2}[CO_2 \cdot \beta] \quad (14)$$

is valid throughout the course of the experiment. The signals for G_{CO} and G_{CO_2} are measured by the mass spectrometer and recorded by the peak programmer as functions of time and thus G_{CO} and G_{CO_2} are known. The pressures or concentrations [CO] and [CO_2] are also known, as is the total amount of adsorbed gas [$CO \cdot \alpha$] + [$CO_2 \cdot \beta$]. The individual amounts of adsorbed gas were estimated from the adsorption data as discussed elsewhere (*2*). The goal of the data-fitting work, then, was to fit the G_{CO} and G_{CO_2} versus time curves using the above equations. The convergence values of R_1, R_2, and R_3 are the equilibrium rates of CO and CO_2 adsorption and desorption and surface interconversion under the conditions of each experiment.

To extract the rate constants from R_1, R_2, and R_3, it is necessary to know the amount of adsorbed CO and CO_2 (i.e., [$CO \cdot \alpha$] and [$CO_2 \cdot \beta$]) and the numbers of α and β sites available on the surface. An alternate model can be derived, however, assuming that adsorbed CO and CO_2 on the surface are indistinguishable; that is, CO and CO_2 form the same species $COO \cdot s$. The reaction equations thus become

$$CO + \alpha \underset{k_1'}{\overset{k_1}{\rightleftarrows}} COO \cdot s \quad (15)$$

$$CO_2 + \beta \underset{k_2'}{\overset{k_2}{\rightleftarrows}} COO \cdot s. \quad (16)$$

This model requires only that the total quantity of adsorbed species be known. The adsorption data of Kubsh *et al.* (*2*) were fit according to this model assuming that the total number of adsorption sites on the surface, θ_{sat}, was a constant and that

$$\theta_{sat} = [\alpha] + [\beta] + [COO \cdot s]. \quad (17)$$

The equilibrium constants for adsorption,

$$K_1 = \frac{[COO \cdot s]}{[CO][\alpha]} \quad (18)$$

$$K_2 = \frac{[COO \cdot s]}{[CO_2][\beta]} \quad (19)$$

were found. At 637 K, $\theta_{sat} = 0.229$, $K_1 = 1.17\ kPa^{-1}$, and $K_2 = 0.38\ kPa^{-1}$.

The data for the isotopic exchange experiment can also be fit using the model of Eqs. (15) and (16). In this case, the expressions include the fraction of total labeled species on the surface A ($A = A_{CO} = A_{CO_2}$). The time-dependent expressions for the isotopic exchange are thus:

$$\frac{d[^{13}CO]}{dt} = [CO]\frac{dG_{CO}}{dt} = R_1(A - G_{CO}) \quad (20)$$

$$\frac{d[^{13}CO_2]}{dt} = [CO_2]\frac{dG_{CO_2}}{dt} = R_2(A - G_{CO_2}) \quad (21)$$

$$\frac{d[^{13}C_{ads}]}{dt} = [C_{ads}]\frac{dA}{dt} = R_1(G_{CO} - A) + R_2(G_{CO_2} - A). \quad (22)$$

In this case [$^{13}C_{ads}$] and [C_{ads}] are the amounts of labeled adsorbed species and total adsorbed species, respectively. If the rates R_1 and R_2 are known, they can be combined with the rate expressions of Eqs. (15) and (16) and the adsorption parameters of expressions (18) and (19) to find the rate constants for adsorption and desorption k_1, k_1', k_2, and k_2'.

Equations (20)–(22) can also be used to fit the data if surface interconversion occurs as in Eqs. (3)–(5) when the rate of surface conversion (Eq. (5)) is rapid relative to the adsorption/desorption rates (Eqs. (3) and (4)). Therefore, a good fit of the data to Eqs. (20)–(22) cannot be taken as proof that a common surface species exists from adsorption of CO and CO_2.

RESULTS AND DISCUSSION

Isotopic Exchange Measurements

When the curves were fit by a least-squares subroutine using the model of Eqs. (11)–(13), it was found that the apparent rate of interconversion on the catalyst surface, R_3, was significantly faster than either R_1 or R_2, the adsorption/desorption rates of CO or CO_2. In general, the values for R_3 were at least an order of magnitude larger than R_1 and R_2. It can, therefore, be concluded that either the interconversion of adsorbed CO and CO_2 on the catalyst surface is fast and in equilibrium relative to the two adsorption rates, or that adsorbed CO and CO_2 are indistinguishable. For simplicity, the model of Eqs. (20)–(22) was, therefore, used to fit the data.

Figure 2 shows a representative set of G_{CO} and G_{CO_2} data. All data sets are given elsewhere (*13*). This particular experiment started with labeled CO_2 and natural CO in the gas phase. The initial value of G_{CO_2} is less than 1.0 because a small amount of natural CO_2 was present initially in the cell in equilibrium with the catalyst. The lag-time before the appearance of the labeled CO in the gas phase was reproducible and was observed for every run where the initial gas mixture consisted of $^{13}CO_2$ and ^{12}CO. For experiments where the initial gas mixture consisted of ^{13}CO and $^{12}CO_2$, a lag-time before the appearance of $^{13}CO_2$ in the gas phase was also observed, as seen in Fig. 3. That a time-lag for interconversion exists is proof that the correct CO–CO_2 interconversion mechanism includes an adsorbed intermediate. This is demonstrated below.

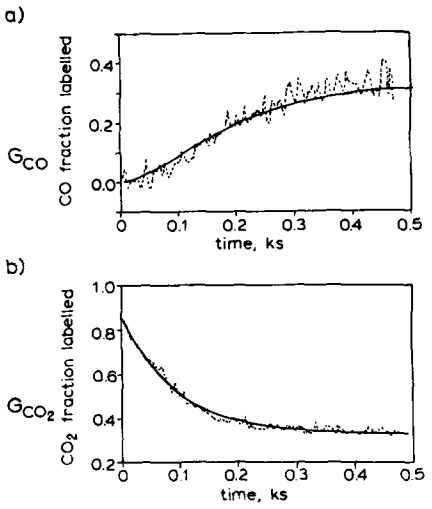

FIG. 2. Fraction of (a) CO and (b) CO_2 labeled as a function of time (CO_2 initially labeled). Shown are calibrated data (---) and best fit according to Eqs. (20)–(22) (—). $R_1 = 0.138$ μmol/s, $R_2 = 0.414$ μmol/s.

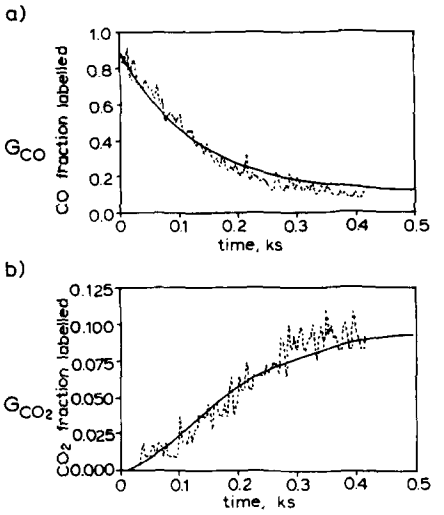

FIG. 3. Fraction of (a) CO and (b) CO_2 labeled as a function of time (CO initially labeled). Shown are calibrated data (---) and best fit according to Eqs. (20)–(22) (—). $R_1 = 0.138$ μmol/s, $R_2 = 0.414$ μmol/s.

The Rideal–Eley form of the regenerative mechanism for CO/CO_2 interconversion is given by the equation

$$CO + O^* \underset{k_r}{\overset{k_f}{\rightleftarrows}} CO_2 + * \qquad (23)$$

where O* represents an oxygen-containing site on the surface and * an anion-vacancy surface site. The rate of interconversion R_x is given by

$$R_x = k_f[CO][O^*] - k_r[CO_2][*], \quad (24)$$

where k_f and k_r are the forward and reverse reaction rate constants. If G_{CO} and G_{CO_2} represent the labeled fractions of gas phase CO and CO_2, respectively, the differential equations for changes in G_{CO} and G_{CO_2} with respect to time are given by

$$-[CO_2]\frac{dG_{CO_2}}{dt} = [CO]\frac{dG_{CO}}{dt} = -G_{CO}k_f[CO][O^*] + G_{CO_2}k_r[CO_2][^*]. \quad (25)$$

If a Rideal–Eley regenerative mechanism were prevailing, the decrease in the labeled fraction of the initially labeled species would be accompanied by a corresponding increase in the labeled fraction of the other gas phase species. This is not the case for any of the experiments of the present study.

The conclusion that adsorbed species are either rapidly interconverting or indistinguishable is further supported by the following result. Two sets of data were collected at essentially the same total pressure, temperature, and composition. For one run, ^{13}CO was the initially labeled gas phase species, and for the other run, $^{13}CO_2$ was the initially labeled gas phase species. Interconversion between CO and CO_2 can be represented as

$$CO(g) \overset{R_1}{\rightleftharpoons} CO(ads) \overset{R_3\ (fast)}{\rightleftharpoons} CO_2(ads) \overset{R_2}{\rightleftharpoons} CO_2(g). \quad (26)$$

Experiments done using ^{13}CO as the initially labeled gas phase species measure R_1 relatively directly, since the initial decrease in G_{CO} is predominantly due to exchange of labeled CO in the gas phase with natural CO on the catalyst surface. The eventual increase in G_{CO_2} through interconversion and subsequent desorption of surface species is used to calculate R_2, assuming that R_3 is fast or that only one surface species exists. If R_3 were not rapid, the calculated value of R_2 would then be lower than the actual adsorption/desorption rate for CO_2. Likewise, if the assumption of rapid interconversion or equivalent adsorbed species is incorrect, then for experiments starting with $^{13}CO_2$ and natural CO, the convergence values for R_2 would be close to the correct value, but the indirectly calculated value of R_1 would be too low.

The results of two experiments run under similar conditions, with different initially labeled species, are given in Table 1. The 2σ confidence limits of R_1 and R_2 values for the two runs are within ±10%. It is thus concluded that the treatment of R_3 as a rapid step relative to R_1 and R_2 is appropriate. The fits for the two sets of data are shown in Figs. 2 and 3.

Table 2 summarizes calculated values of R_1 and R_2 under different experimental conditions on different catalyst samples. The BET monolayer capacities (μmol N_2 adsorbed at 77 K) of the four samples are different. Also, the gas phase compositions, temperatures, pressures, and total uptakes of CO and CO_2 by the catalyst vary. However, thermodynamic calculations can be used to show that these results are self-consistent.

Since the system is at equilibrium, the adsorption equilibrium constants for CO and CO_2 from Eqs. (3) and (4) can be written:

$$K_1 = \frac{[CO \cdot \alpha]}{[CO][\alpha]} \quad (27)$$

$$K_2 = \frac{[CO_2 \cdot \beta]}{[CO_2][\beta]}. \quad (28)$$

TABLE 1

Comparison between ^{13}CO and $^{13}CO_2$ as Initially Labeled Species

Initially labeled species:	CO	CO_2
Conditions of experiment		
N_{CO} (μmol)	18.65	20.37
N_{CO_2} (μmol)	67.62	62.54
G_{CO}	0.893	0
G_{CO_2}	0	0.900
N_{ads} (μmol)	78.81	81.81
T (K)	627	630
P (kPa)	2.55	3.01
P (Torr)	19.1	22.6
Results		
R_1 (μmol/s)	0.138	0.155
R_2 (μmol/s)	0.414	0.466

TABLE 2

Results of Exchange Experiments

T (K)	P (kPa)	P (Torr)	y_{CO}	Sample[a]	BET monolayer (μmol N_2, 77 K)	N_{ads} (μmol)	R_1	R_2	R_1 (10^{-4} μmol/ μmol BET s)	R_2	R_2/R_1	Initially labeled species
							μmol/s					
627	2.55	19.1	0.23	A	798	78.81	0.138	0.414	1.73	5.19	3.00	CO
627	2.21	16.6	0.17	B	740	102.96	0.345	0.833	4.66	11.24	2.41	CO
593	2.51	18.8	0.29	D	615	90.03	0.245	0.560	3.98	9.11	2.29	CO
568	2.13	16.0	0.25	B	740	142.77	0.165	2.951	2.23	39.85	17.89	CO
568	2.46	18.5	0.17	B	732	135.98	0.114	1.984	1.56	27.10	17.40	CO
630	3.01	22.6	0.21	A	798	81.81	0.155	0.466	1.94	5.84	3.01	CO_2
627	2.35	17.6	0.08	C	541	62.42	0.358	0.845	6.62	15.62	2.36	CO_2
627	3.22	24.2	0.14	C	541	57.58	0.190	0.696	3.51	12.87	3.66	CO_2
627	2.99	22.4	0.28	C	541	62.51	0.237	0.486	4.38	8.98	2.05	CO_2
563	2.44	18.3	0.07	B	732	137.17	0.0926	1.527	1.25	20.61	16.49	CO_2

[a] A—1.9 g, unsieved; BET monolayer = 798 μmol N_2. B—1.9 g, 70–100 mesh; BET monolayer = 740 μmol. C—1.6 g, finer than 200 mesh; BET monolayer = 541 μmol. D—1.9 g, 70–100 mesh; BET monolayer = 615 μmol.

The equilibrium constant for surface interconversion of the adsorbed species is

$$K_3 = \frac{[CO_2 \cdot \beta]}{[CO \cdot \alpha]}. \qquad (29)$$

We can then define the rate ratio R_2/R_1 by combining Eqs. (27)–(29) to obtain

$$\frac{R_2}{R_1} = \frac{k_2'[CO_2 \cdot \beta]}{k_1'[CO \cdot \alpha]} = \frac{k_2'K_3}{k_1'}. \qquad (30)$$

Therefore, at a given temperature, the rate ratio R_2/R_1 should be constant, independent of gas phase composition. A plot of R_2/R_1 at different gas compositions is given in Fig. 4. It is clear that the rate ratio depends neither on the gas composition nor on whether the initially labeled species was CO or CO_2. If adsorbed CO and CO_2 form an indistinguishable surface species, as in Eqs. (15) and (16), it can be shown that

$$\frac{R_2}{R_1} = \frac{k_2'}{k_1'} \qquad (31)$$

and the constant rate ratio is still expected. Figure 4 shows that at 627 K, the equilibrium rate of CO_2 adsorption/desorption is 2.4 times as fast as the rate for CO. At 568 K, however, there is a much larger difference in the relative rates, and the adsorption/desorption rate of CO_2 is 17 times as fast as that for CO.

Since a model where CO and CO_2 are indistinguishable once adsorbed on the surface is consistent with the experimental data of this study, it will be assumed below that this adsorbed species might be a bidentate carbonate. First, it is not reasonable to assume that CO will interact quickly with the surface to form a bidentate carbonate. The bidentate carbonate is believed to be an activated form of adsorbed CO which is evolved from weakly adsorbed carbonyl species (*15–18*). Thus, a reasonable sequence for interconversion of CO and CO_2 would be

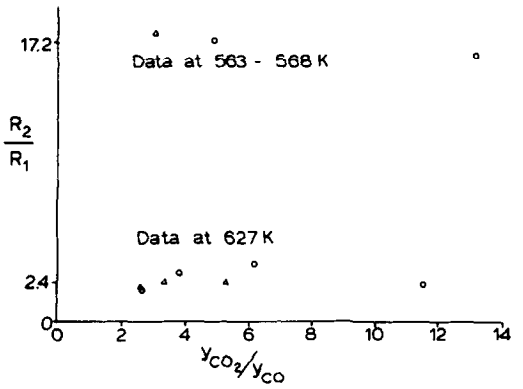

FIG. 4. Plot of R_2/R_1 vs composition. (○) CO_2 initially labeled, (△) CO initially labeled.

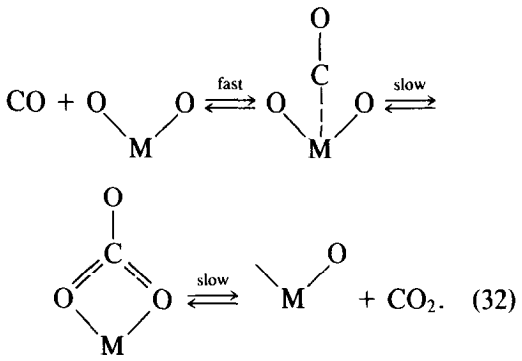

The first interaction of the CO is with a surface cation (*18*). This weak interaction can be fast and still be in agreement with the present results if there is only a small amount of this species on the surface relative to the number of bidentate carbonate species. Thus, R_1 could correspond to the equilibrium rate of conversion between the carbonyl and bidentate carbonate forms of adsorbed CO.

If adsorbed CO and CO_2 form a common adsorbed species, COO · s, as in Eqs. (15) and (16), the mass balance requires that an α site (for CO adsorption) be a β site (for CO_2 adsorption) with an additional oxygen available. Therefore, the ratio of sites containing an oxygen vacancy to sites from which an oxygen can be removed is given by $[\alpha]/[\beta]$. If CO and CO_2 adsorb to form a common adsorbed species, from Eqs. (18) and (19) it follows that:

$$\frac{[\alpha]}{[\beta]} = \frac{K_2[CO_2]}{K_1[CO]}. \tag{33}$$

Indeed, Kubsh (*1*, *3*) showed experimentally that the ratio of oxygen-containing to anion-vacancy sites on the surface depends on the $[CO_2]/[CO]$ ratio in the gas phase.

The rates measured by isotopic exchange in the present study can be combined with the adsorption data of Kubsh *et al.* (*2*) to estimate rate constants for the adsorption and desorption of CO and CO_2. The adsorption models most consistent with the data are the model given by Eqs. (3)–(5), which involves a rapid interconversion of CO and CO_2, and the model given by Eqs. (15) and (16), where CO and CO_2 adsorb on different sites as a common species. Since equilibrium constants for adsorption can be calculated unambiguously only for the latter model, it will be used to calculate rate constants from the data of this study.

For the model of Eqs. (15) and (16), the measured exchange rates of R_1 and R_2 can be related to the rate constants by

$$R_1 = k_1[CO][\alpha] = k_1'[COO \cdot s] \tag{34}$$

$$R_2 = k_2[CO_2][\beta] = k_2'[COO \cdot s]. \tag{35}$$

The total uptake [COO · s] for each experimental run is known. Values of k_1' and k_2' for experiments carried out at 627 K calculated from the above relationships are tabulated in Table 3.

Values for k_1 and k_2 were calculated from the expressions

$$K_1 = \frac{k_1}{k_1'} \tag{36}$$

$$K_2 = \frac{k_2}{k_2'} \tag{37}$$

using the mean values of k_1' and k_2' from Table 3 and $K_1 = 1.17\ kPa^{-1}$ and $K_2 = 0.38\ kPa^{-1}$. The rate constants k_1 and k_1' are therefore $3.9 \times 10^{-3}\ kPa^{-1}\ s^{-1}$ and $3.3 \times 10^{-3}\ s^{-1}$, respectively, and k_2 and k_2' are determined to be $3.3 \times 10^{-3}\ kPa^{-1}\ s^{-1}$ and $8.7 \times 10^{-3}\ s^{-1}$, respectively.

TABLE 3

Rate Constants Calculated from Isotopic Exchange Data at 627 K

P_T (kPa)	P_T (Torr)	y_{CO}	[COO · s] (μmol)	R_1	R_2	k_1'	k_2'
				μmol/s		$\times 10^{-3}\ s^{-1}$	
2.21	16.6	0.17	102.96	0.345	0.833	3.35	8.01
2.55	19.1	0.23	78.81	0.138	0.414	1.75	5.25
3.22	24.2	0.14	57.58	0.190	0.696	3.30	12.09
2.99	22.4	0.28	62.51	0.237	0.486	3.79	7.77
2.35[a]	17.6	0.08	62.42	0.358	0.845	5.74	13.54
3.01[b]	22.6	0.21	81.81	0.155	0.466	1.89	5.70

[a] Not included in averaging because of strong dependence on the y_{CO} measurement, which includes greater error at high CO_2 : CO ratios.

[b] Actual temperature = 630 K.

Implications for Kinetics of Water-Gas Shift

The results of the above isotopic exchange experiments show that the interconversion of CO and CO_2 through interaction with the catalyst surface occurs through an adsorbed intermediate. The results also show either that the interconversion on the surface is rapid and in equilibrium relative to the CO and CO_2 adsorption, or that a single species predominates on the surface which results from adsorption of either CO or CO_2. Based on the latter case, rate constants for adsorption and desorption of CO and CO_2 were calculated from the isotopic exchange data. These rate constants will now be used in a mechanistically based kinetic model of water-gas shift. In using these rate constants, it will be assumed that the rate constants and mechanism of CO–CO_2 interconversion are not affected by the presence of adsorbed H_2 and H_2O. In the present case, only competition for adsorption sites will be considered.

The scheme of interconversion between CO and CO_2 through a bidentate carbonate given by Eq. (32) is proposed to represent the catalytic interconversion of CO and CO_2 during water-gas shift. A possible route for H_2–H_2O interconversion is given by

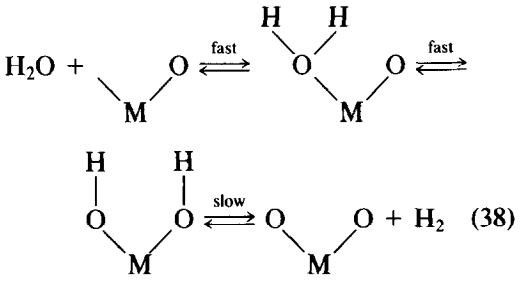

(38)

where M is a surface cation and O represents surface oxygen. The desorption of H_2 has been chosen to be the slow step of this process in view of the findings by Oki and co-workers (*19–25*). If α is now used to represent a M—O pair-site and an adjacent surface oxygen, and β is used to represent a M—O pair-site with an adjacent vacant site, the above schemes can be rewritten as

$$\begin{aligned}
&\text{(i) slow} && \mathrm{CO} + \alpha \rightleftarrows \mathrm{COO \cdot s} \\
&\text{(ii) slow} && \mathrm{COO \cdot s} \rightleftarrows \mathrm{CO_2} + \beta \\
&\text{(iii) fast} && \mathrm{H_2O} + \beta \rightleftarrows \mathrm{H_2O \cdot \beta} \\
&\text{(iv) fast} && \mathrm{H_2O \cdot \beta} + \alpha \rightleftarrows 2\mathrm{H}\alpha \\
&\text{(v) slow} && 2\mathrm{H}\alpha \rightleftarrows \mathrm{H_2} + 2\alpha.
\end{aligned} \tag{39}$$

The initial weak interaction of CO with the surface has not been included because, as was discussed previously, it is assumed not to be kinetically significant. A rate expression derived from this model, even assuming that steps (iii) and (iv) are in equilibrium, would be very complex because of the second-order terms in steps (iv) and (v). This particular mechanism, however, is consistent with the available data.

For purposes of simplification, the dissociative adsorption of hydrogen will be disregarded. This simplification is justified on the basis of the small extent of hydrogen which is likely to be adsorbed under reaction conditions (*26*). Furthermore, because of their small size, surface hydrogen atoms (or protons) are not expected to block adsorption sites for CO, CO_2, and H_2O.

Accordingly, the above model is simplified as follows:

$$\begin{aligned}
&\text{(i) slow} && \mathrm{CO} + \alpha \underset{k_1'}{\overset{k_1}{\rightleftarrows}} \mathrm{COO \cdot s} \\
&\text{(ii) slow} && \mathrm{COO \cdot s} \underset{k_2}{\overset{k_2'}{\rightleftarrows}} \mathrm{CO_2} + \beta \\
&\text{(iii) fast} && \mathrm{H_2O} + \beta \underset{k_3'}{\overset{k_3}{\rightleftarrows}} \mathrm{H_2O \cdot s} \\
&\text{(iv) slow} && \mathrm{H_2O \cdot s} \underset{k_4}{\overset{k_4'}{\rightleftarrows}} \mathrm{H_2} + \alpha
\end{aligned} \tag{40}$$

where k_n and k_n' are the rate constants for adsorption and desorption of each species, α and β represent M—O pair-sites with and without surface oxygen, respectively, and

K_n are the equilibrium constants for each adsorption process. Because step (iii) is assumed to be in equilibrium,

$$[H_2O \cdot s] = K_3[H_2O][\beta]. \quad (41)$$

Bracketed gas phase species again represent concentrations and bracketed surface species the numbers of adsorbed surface species. The rate of reaction for the above scheme is given by the rate of step (i):

$$R = -\frac{d[CO]}{dt} = k_1[CO][\alpha] - k_1'[COO \cdot s]. \quad (42)$$

Using steady-state assumptions for adsorbed species and a balance of sites on the surface, expressions for $[\alpha]$ and $[COO \cdot s]$ can be developed in terms of concentrations of gas phase species, adsorption rate contants, and equilibrium constants. It then follows that

$$R = \frac{\left(\frac{k_1k_2'K_3k_4'}{k_1' + k_2'}[CO][H_2O] - \frac{k_1'k_2k_4}{k_1' + k_2'}[CO_2][H_2]\right) n_{sat}}{\left[\left(1 + \frac{k_2[CO_2]}{k_1' + k_2'} + K_3[H_2O]\right)\left(\frac{k_1k_2'}{k_1' + k_2'}[CO] + k_4[H_2]\right) + \left(1 + \frac{k_1[CO]}{k_1' + k_2'}\right)\left(\frac{k_1'k_2}{k_1' + k_2'}[CO_2] + K_3k_4'[H_2O]\right)\right]} \quad (43)$$

where n_{sat} is the number of surface sites per unit area that are active for adsorption processes and water-gas shift (*3*). This equation is a Langmuir–Hinshelwood–Hougen–Watson model for reaction occurring on two sites. The expression

$$1 + \frac{k_2}{k_1' + k_2'}[CO_2] + K_3[H_2O]$$

represents competitive adsorption on β sites. Carbon monoxide also competes for these sites but it is not present in the equation because its initial adsorption was assumed to be weak. The term

$$\frac{k_1k_2'}{k_1' + k_2'}[CO] + k_4[H_2]$$

represents the generation of β sites from reaction of CO and H_2 with α sites. The term

$$\frac{k_1'k_2}{k_1' + k_2'}[CO] + K_3k_4'[H_2O]$$

is similarly the rate of formation of α sites from the reaction of CO_2 and H_2O with β sites, and adsorption on α sites results in the term

$$1 + \frac{k_1}{k_1' + k_2'}[CO].$$

A further simplification can be made based on the known small extent of hydrogen adsorption (*26*). Therefore, it will be assumed that $k_4[H_2]$ is small relative to the other terms in the denominator of the rate expression. This assumption is consistent with the result of Bohlbro (*27*) and others (*28*) that the forward rate of water-gas shift is independent of hydrogen concentration. Dropping the term for the reverse reaction and assuming that the H_2 adsorption term is negligible, Eq. (43) reduces to

$$R = \frac{\left(\frac{k_1k_2'K_3k_4'}{k_1' + k_2'}[CO][H_2O]n_{sat}\right)}{\left[\left(1 + \frac{k_2[CO_2]}{k_1' + k_2'} + K_3[H_2O]\right)\left(\frac{k_1k_2'}{k_1' + k_2'}[CO]\right) + \left(1 + \frac{k_1[CO]}{k_1' + k_2'}\right)\left(\frac{k_1'k_2}{k_1' + k_2'}[CO_2] + K_3k_4'[H_2O]\right)\right]}. \quad (44)$$

The values of k_1, k_1', k_2, and k_2' were calculated from the results of the isotopic exchange experiment. The value of the adsorption equilibrium constant for water, K_3, can be determined from H_2/H_2O adsorption isotherms (*26*). The desorption rate con-

stant for H_2, k_4', cannot be determined directly, but it was estimated as described below.

Oki and Mezaki (*19*) estimated the rates of CO and H_2 adsorption and desorption on Fe_2O_3 at 673 K. The rate of desorption of H_2 was calculated to be approximately 2.5 times the rate of desorption of CO for equal pressures of CO, CO_2, H_2, and H_2O. According to Eq. (40), it follows that

$$k_4'[H_2O \cdot s] \cong 2.5k_1'[COO \cdot s]. \quad (45)$$

Near equilibrium it can also be written that

$$[COO \cdot s] \cong K_1[CO][\alpha] \quad (46)$$

$$[H_2O \cdot s] \cong K_3[H_2O][\alpha]. \quad (47)$$

Thus, for the equal pressures of H_2O and CO used by Oki and Mezaki (19),

$$k_4' \cong 2.5k_1' \frac{K_1}{K_3} \quad (48)$$

and k_4' is estimated to be 3.2×10^{-2} s^{-1}.

TABLE 4

Rate Constants and Equilibrium Constants Used to Predict the Rate of Water-Gas Shift over Chromia-Promoted Magnetite at 627 K Using Eq. (44)

Symbol	Value	Definition	Source
k_1	3.9×10^{-3} kPa^{-1} s^{-1}	CO adsorption rate constant	Combined ads. data (*2*) with isotopic exchange data
k_1'	3.3×10^{3} s^{-1}	CO desorption rate constant	Combined ads. data (*2*) with isotopic exchange data
K_1	1.17 kPa^{-1}	CO adsorption equilibrium constant	Adsorption data (*2*)
k_2	3.3×10^{-3} kPa^{-1} s^{-1}	CO_2 adsorption rate constant	Combined ads. data (*2*) with isotopic exchange data
k_2'	8.7×10^{-3} s^{-1}	CO_2 desorption rate constant	Combined ads. data (*2*) with isotopic exchange data
K_2	0.38 kPa^{-1}	CO_2 adsorption equilibrium constant	Adsorption data (*2*)
K_3	0.3 kPa^{-1}	H_2O adsorption equilibrium constant	Adsorption data (*26*)
k_4'	3.2×10^{-2} s^{-1}	H_2 desorption rate constant	Estimated by combining data of Oki and Mezaki (*19*), adsorption data (*2*, *26*), and isotopic exchange data
n_{sat}	1.25×10^{18} m^{-2}	Number of sites per surface area	Adsorption data (*2*, *26*)

This estimate assumes that the temperature effects between 673 and 627 K for CO and H_2 desorption are equal.

The values of the equilibrium and rate constants used in the model of Eq. (44), as well as their sources, are listed in Table 4.

Water-gas shift rates calculated using the rate contants of Table 4 and Eq. (44) are plotted in Fig. 5. The rates predicted from the present model are compared to rates calculated from the power law as fit by Bohlbro (*27*) which at 627 K has the form

$$R = 3.6 \times 10^{15} P_{CO}^{0.9} P_{H_2O}^{0.25} P_{CO_2}^{-0.65}, \quad (49)$$

where R has the units $m^{-2}\ s^{-1}$ and P_i have units of kPa. The P_i are set equal to 10 kPa (75 Torr) as a basis for comparison, since the adsorption data as well as the data of Bohlbro were collected in this pressure range. The isotopic exchange data of the present study and the data of Oki and Mezaki (*19*) were collected at pressures approximately an order of magnitude lower. If the pressure of each species is set equal to 10 kPa, Eq. (44) predicts a forward reaction rate of $6.0 \times 10^{15}\ m^{-2}\ s^{-1}$ while the expression of Bohlbro predicts a rate of $11.38 \times 10^{15}\ m^{-2}\ s^{-1}$. This agreement is good.

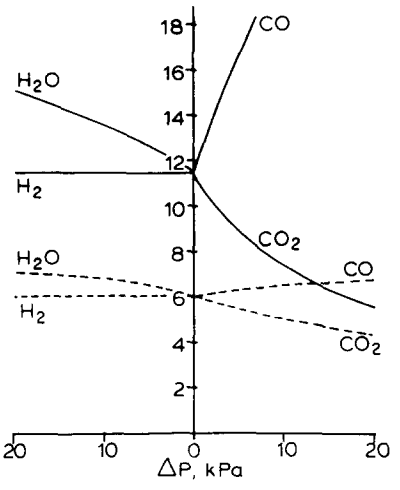

FIG. 5. The forward rate of water-gas shift at 627 K as predicted by Eq. (44) (---), and compared to the rate calculated from Bohlbro's rate expression (—). The effect of individually increasing the partial pressure of each component from 10 to 30 kPa is given by ΔP ($\Delta P = 0$ corresponds to all $P_i = 10$ kPa).

One of the assumptions which might affect the predicted reaction rate is the assumption that CO_2 and H_2O are competing for sites. If formate or bicarbonate species are present on the surface, the adsorption sites are actually shared to some extent. The present model, for the sake of simplicity, assumes that there are only two species present on the surface: one resulting from the interaction of CO or CO_2 and one from the interaction of H_2 or H_2O. Furthermore, the adsorption characteristics of CO and CO_2 might be different in the presence of H_2 and H_2O. The rate constants calculated from the isotopic exchange and the adsorption data do not predict the result of Oki and co-workers (*19–25*) that the adsorption/desorption of CO_2 is fast compared to the adsorption/desorption of H_2 and CO. It might be possible that the activation energy of adsorption of CO_2 is lower in the presence of H_2 and H_2O and the adsorption/desorption rates are higher than those calculated from the isotopic exchange data.

CONCLUSIONS

The results of the isotopic exchange experiments indicate that interconversion of CO and CO_2 is rapid relative to the adsorption and desorption of either species or that a common adsorbed species results from the adsorption of CO and CO_2. Assuming the existence of a single adsorbed species, the results of the isotopic exchange experiments were combined with CO/CO_2 adsorption data of Kubsh *et al.* (*2*) to obtain rate constants for adsorption and desorption.

A mechanism for the water-gas shift reaction was proposed that is consistent with the results of the isotopic exchange experiments. The mechanism was used to derive a kinetic rate expression. The rate constants calculated from the isotopic exchange results and equilibrium constants from adsorption isotherm data were used in the kinetic rate expression to predict the water-gas shift reaction rate. Although the mechanistic model predicted a weaker de-

pendence of the rate on the pressures of the individual species than observed experimentally, the trends are in qualitative agreement. It is proposed that the mechanism of Eq. (32) is a reasonable representation of the $CO-CO_2$ interconversion through surface oxygen exchange with the catalyst under water-gas shift conditions.

ACKNOWLEDGMENTS

We wish to thank the National Science Foundation for the financial support of this work and for providing a Graduate Fellowship for one of us (M.T.). We also wish to thank Professor W. E. Stewart and D. Weidman for their invaluable assistance in fitting the isotopic exchange data. Valuable discussions with C. R. F. Lund, J. E. Kubsh, and D. Rethwisch are also acknowledged.

REFERENCES

1. Lund, C. R. F., Kubsh, J. E., and Dumesic, J. A., *in* "Solid State Chemistry in Catalysis" (R. K. Graselli and J. F. Bradzil, Eds.), ACS Symp. Ser. No. 279, p. 313. Amer. Chem. Soc., Washington, D.C., 1985.
2. Kubsh, J. E., Chen, Y., and Dumesic, J. A., *J. Catal.* **71,** 192 (1981).
3. Kubsh, J. E., and Dumesic, J. A., *AIChE J.* **28,** 793 (1982).
4. Kodama, S., Fukui, K., Tame, T., and Kinoshita, M., *Shokubai* **8,** 50 (1952).
5. Temkin, M. I., Nakhmanovich, M. L., and Morozov, N. M., *Kinet. Katal.* **2,** 722 (1961).
6. Rethwisch, D. G., and Dumesic, J. A., *Appl. Catal.* **21,** 97 (1986).
7. Wagner, C., *Ber. Bunsenges. Phys. Chem.* **74,** 401 (1970).
8. Wagner, C., *in* "Advances in Catalysis" (D. D. Eley, H. Pines, and P. B. Weisz, Eds.), Vol. 21, p. 323. Academic Press, New York, 1970.
9. Lund, C. R. F., and Dumesic, J. A., *J. Catal.* **76,** 93 (1982).
10. Muan, A., and Osborn, E. F., "Phase Equilibria among Oxides in Steelmaking." Addison-Wesley, Reading, Mass., 1965.
11. Lund, C. R. F., Schorfheide, J. J., and Dumesic, J. A., *J. Catal.* **57,** 105 (1979).
12. Rethwisch, D. G., and Dumesic, J. A., *Langmuir* **2,** 73 (1986).
13. Tinkle, M., Ph.D. thesis. University of Wisconsin, Madison, 1985.
14. Kobal, I., Senegacnik, M., and Kobal, H., *J. Chem. Phys.* **78,** 1815 (1983).
15. Rubene, N. A., Davydov, A. A., Kravtsov, A. V., Usheva, N. V., and Smol'yaninov, S. I., *Kinet. Katal.* **17,** 465 (1976).
16. Kasatkina, L. A., Nekipelov, V. N., and Zhivotenko, N. N., *Kinet. Katal.* **14,** 363 (1973).
17. Viswanathan, B., Krishamurthy, K. R., and Sastri, M. V. C., *J. Res. Inst. Catal., Hokkaido Univ.* **27,** 79 (1979).
18. Udovic, T. J., and Dumesic, J. A., *J. Catal.* **89,** 314 (1984).
19. Oki, S., and Mezaki, R., *J. Phys. Chem.* **77,** 1601 (1973).
20. Kaneko, Y., and Oki, S., *J. Res. Inst. Catal., Hokkaido Univ.* **13,** 55 (1965).
21. Kaneko, Y., and Oki, S., *J. Res. Inst. Catal., Hokkaido Univ.* **13,** 169 (1965).
22. Kaneko, Y., and Oki, S., *J. Res. Inst. Catal., Hokkaido Univ.* **15,** 185 (1967).
23. Oki, S., Happel, J., Hnatow, M., and Kaneko, Y., *in* "Proceedings, 5th International Congress on Catalysis, Palm Beach, 1972" (J. Hightower, Ed.), Vol. 1, pp. 173–182. North-Holland, Amsterdam, 1973.
24. Oki, S., and Mezaki, R., *J. Phys. Chem.* **77,** 447 (1973).
25. Mezaki, R., and Oki, S., *J. Catal.* **30,** 488 (1973).
26. Tinkle, M., and Dumesic, J. A., *J. Phys. Chem.* **88,** 4127 (1984).
27. Bohlbro, H., "An Investigation on the Kinetics of the Conversion of Carbon Monoxide with Water Vapour over Iron Oxide Based Catalysts," 2nd ed. Haldor Topsøe, Gjellerup, Copenhagen, 1969.
28. Podolski, W. F., and Kim, Y. G., *Ind. Eng. Chem., Proc. Des. Dev.* **13,** 415 (1974).